

# Fabrication and Rate Performance of Spherical LiFePO<sub>4</sub> Nanoparticles for High-power Lithium Ion Battery

Bing Huang<sup>1,2,\*</sup>, Xiaodong Zheng<sup>1</sup>, Mi Lu<sup>1</sup>, Yiming Zhou<sup>2</sup>, Yu Chen<sup>2</sup>, Su Dong<sup>1</sup> and Yu Qiao<sup>1</sup>

<sup>1</sup>Clean Energy Research and Development Center, Binzhou University, Binzhou, Shandong 256603, China

<sup>2</sup>Jiangsu Key Laboratory of New Power Batteries, Nanjing, Jiangsu 210046, China

Received: September 12, 2011, Accepted: November 14, 2011, Available online: January 23, 2012

**Abstract:** The spherical LiFePO<sub>4</sub>/C nanoparticles are synthesized by modified carbothermal reduction method. XRD patterns show that the LiFePO<sub>4</sub> compound is orthorhombic crystal structure. SEM and TEM results indicate that the LiFePO<sub>4</sub> composite had a spherical morphology with carbon coated and the particle size is nanoscale. Charge/discharge tests and CV curves show that as-prepared sample exhibits discharge capacity of 153 mAh g<sup>-1</sup> at 0.2 C rate with high electrode reaction reversibility. The discharge capacities of the material are 150, 132, 119, 111, 103 and 96 mAh g<sup>-1</sup> at 1 C, 5 C, 10 C, 15 C, 20 C and 25 C rate and high voltage plateaus are achieved. The good rate performance of the composite is due to its nano particle size and spherical morphology, which reduced the diffusion path of lithium ions and electrons, increased the conductive specific surface and improved the processability of the LiFePO<sub>4</sub> cathode.

**Keywords:** Lithium-ion batteries, Cathode materials, LiFePO<sub>4</sub>, Rate performance

## 1. INTRODUCTION

Lithium-ion batteries (LIBs) are the dominant power sources for electronic devices. They are also the most promising candidate for electric vehicles (EVs) and hybrid electric vehicles (HEVs). But new applications in EVs and HEVs require a higher charge-discharge rate capability [1]. The development of cathode materials with good capacity and capacity retention at high rates is critical in improving the power of a LIB system [2–4]. Recently, orthorhombic structure LiFePO<sub>4</sub> powders have become a favorable cathode material because of their low cost, high discharge potential, large specific capacity, good thermal stability, long cycle life and environmental compatibility. However, LiFePO<sub>4</sub> suffers from poor high-rate capacity due to the low electronic conductivity and slow diffusion of lithium ions [5–7]. Tremendous efforts have been made to overcome the inherent limitations of LiFePO<sub>4</sub>. It has been proved that reducing particles to nanometer scale can shorten the lithium ion transport distances and enhance ionic diffusion rate [2, 6, 8–10]. In addition, coating the particles with carbonaceous conductors [11–15] and doping of metallic elements [7, 16–20] are effective ways to improve the electronic conductivity.

Here we report on our work to improve the rate performance of LiFePO<sub>4</sub> materials by making this material spherical nanostructured and carbon coated using modified carbothermal reduction method. Furthermore, Fe (III) raw material is used for Fe, which is relatively cheap and chemically stable compared with Fe(II) compounds, and two types of carbon sources are used as the reducing agent.

## 2. EXPERIMENTAL

The stoichiometric amount of FePO<sub>4</sub>·4H<sub>2</sub>O (99.5%) and Li<sub>2</sub>CO<sub>3</sub> (99.9%) were dispersed in deionized water and then ball milled for the first time for 15 h. The mixtures were dried at 100 °C, and then transferred into a tube furnace and heated to 350 °C for 3 h, under the mixed gas flow (90% Ar + 10% H<sub>2</sub>). Then the pre-calcinated mixtures and the carbon precursors consisted of sucrose and high-surface-area carbon black (18 wt. % and 3 wt. % compared to the LiFePO<sub>4</sub>, respectively) were ball milled again in ethanol for 15 h. The ball-milled mixtures were dried through exposure to vacuum (–0.9 MPa) at 100 °C, and then heated to 700 °C at a heating rate of 5 °C min<sup>-1</sup> for 10 h under mixed gas atmosphere (90% Ar + 10% H<sub>2</sub>).

The obtained LiFePO<sub>4</sub>/C powder was subjected to X-ray diffrac-

\*To whom correspondence should be addressed: Email: huangbingzhu@sina.com  
Fax: +86 (543) 3195583

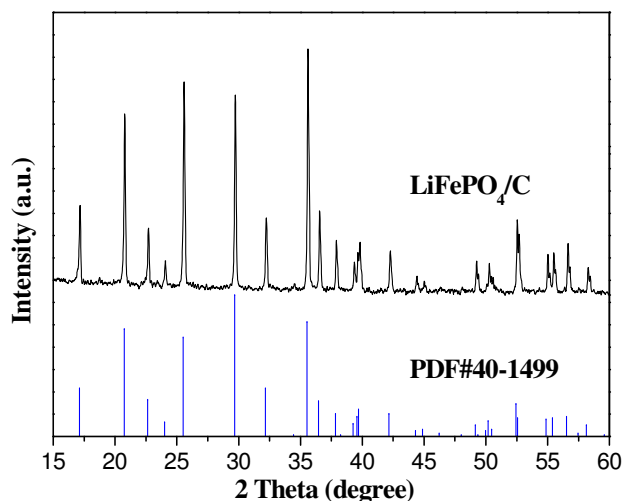


Figure 1. XRD pattern of the  $\text{LiFePO}_4/\text{C}$  composite.

tion (XRD, Analytical X' Pert, Philips) for phase analysis using  $\text{CuK}_\alpha$  radiation. The morphology of the  $\text{LiFePO}_4/\text{C}$  powder was observed by scanning electron microscope (SEM, EM3200, KYKY). The nature and thickness of the coated carbon was measured using the images from a high-resolution transmission electron microscope (HR-TEM, JEM-2100, JEOL).

The  $\text{LiFePO}_4$  slurry was prepared via mixing 80 wt. % active material, 10 wt. % carbon black and 10 wt. % polyvinylidene fluoride solution in N-methylpyrrolidone and then was coated onto an aluminum foil over an area of  $1 \text{ cm}^2$ . The cells (CR2025 coin type) were assembled in an argon-filled glove box (Etelux). The electrolyte was  $1 \text{ mol L}^{-1}$   $\text{LiPF}_6$  in ethylene carbonate/diethylene carbonate/methyl ethyl carbonate (1:1:1, v/v/v) (Ferro). The cells were measured using Neware galvanostatic charge–discharge unit in the voltage range of 2.5–3.9 V. Cyclic voltammetry (CV) was performed with electrochemical instrument (CHI604C, Chenhua).

### 3. RESULTS AND DISCUSSION

Figure 1 shows the X-ray diffraction patterns of the prepared powder. All peaks of the prepared  $\text{LiFePO}_4$  are indexed to an orthorhombic olivine-type structure (space group  $Pnma$ ), in good agreement with the standard PDF Card (No. 40-1499). Excess carbon left in  $\text{LiFePO}_4/\text{C}$  composite was not detected because the residual carbon is amorphous or the thickness of the residual carbon on the  $\text{LiFePO}_4$  powders is too thin [21].

SEM images of  $\text{LiFePO}_4/\text{C}$  sample are shown in figure 2. Figure 2a shows that the as-prepared powders had a homogeneous spherical morphology. The enlarged image is shown in figure 2b, which indicates that the spherical particle was nanoscale in diameter and some flocky solid carbon was embedded in the particles. Since solid carbon is used as the reducing agent, it is important to keep all reactants in good contact with each other throughout the reaction. To further investigate the carbon distribution in the powders, HR-TEM image was taken and shown in figure 2c. The image shows that the thickness of the coated carbon layer is about 3–4 nm. TEM analysis shows the presence of a thin web of carbon surrounding

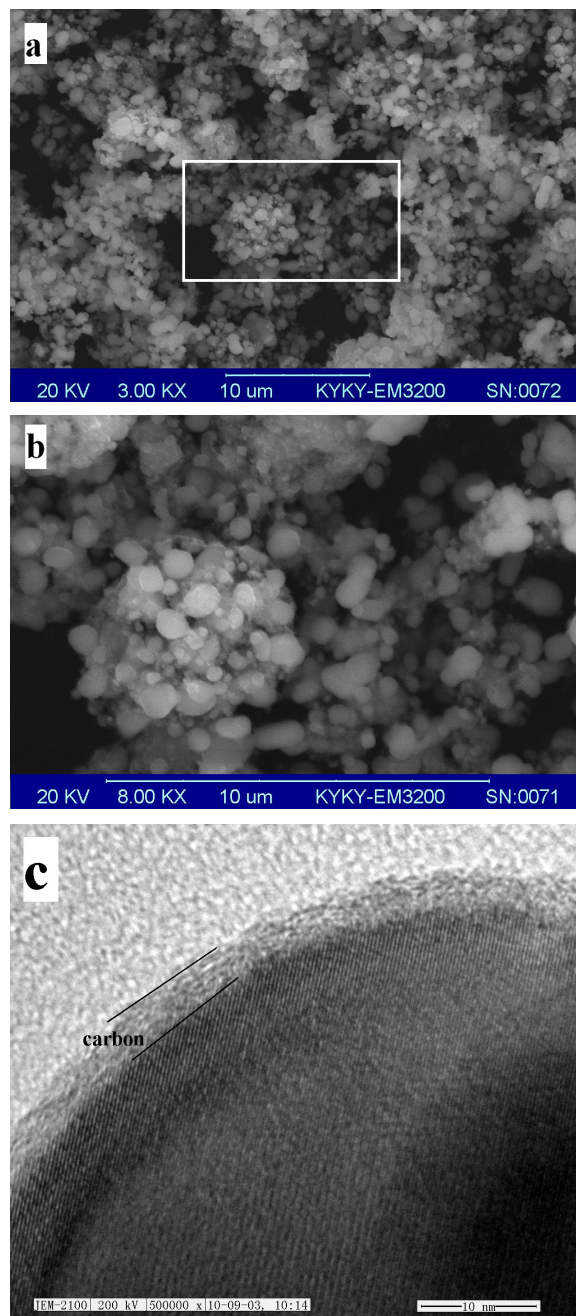


Figure 2. SEM (a) (b) and TEM (c) images of the  $\text{LiFePO}_4/\text{C}$  composite.

the particles. The results showed that the inter-particle agglomeration was reduced by the coated carbon on the surface of  $\text{LiFePO}_4$  particles, which is due to the effective mixing of the carbon sources with the precursors during the ball milling after pre-calcinating the raw materials.

Figure 3 displays the charge–discharge behavior of the  $\text{LiFePO}_4$  electrode operating at 0.2 C rate. The  $\text{LiFePO}_4$  sample exhibits a flat and long voltage plateau at  $\sim 3.4 \text{ V}$ , which indicates the two-phase redox reaction proceeds via a first-order transition between

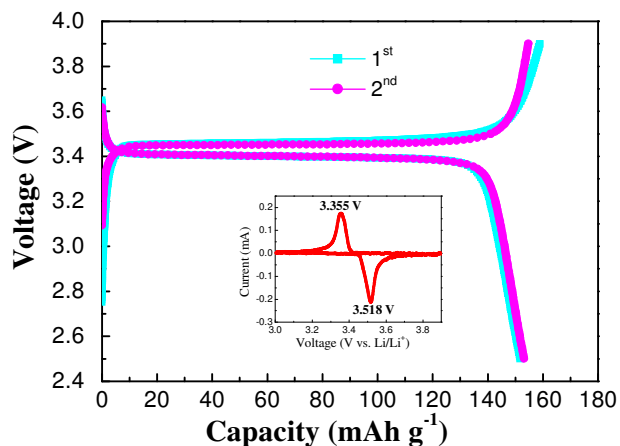


Figure 3. Charge/discharge profiles of the  $\text{LiFePO}_4/\text{C}$  electrode at 0.2 C rate in the voltage range of 2.5–3.9 V (1 C =  $170 \text{ mA g}^{-1}$ ). The insert shows the cyclic voltammetry profile of  $\text{LiFePO}_4/\text{C}$  electrode.

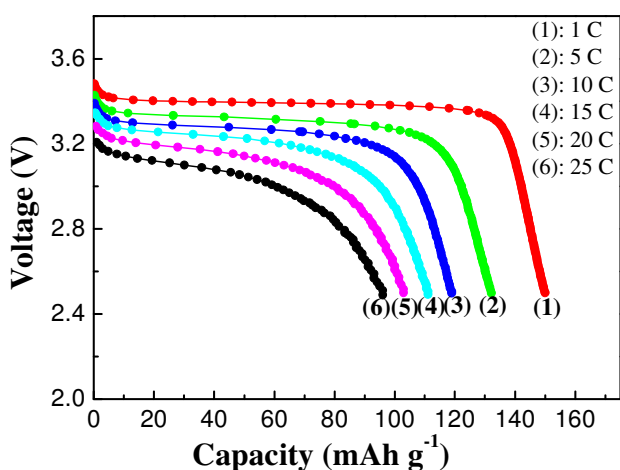


Figure 4. Initial discharge curves of  $\text{LiFePO}_4/\text{C}$  electrode at different rates.

$\text{LiFePO}_4$  and  $\text{FePO}_4$  [5]. The initial charge and discharge capacity of  $\text{LiFePO}_4$  present  $159$  and  $152 \text{ mAh g}^{-1}$ , respectively. And the coulombic efficiency in the first cycle is 95.6%. In the second cycle, the charge capacity of  $\text{LiFePO}_4$  is  $154 \text{ mAh g}^{-1}$  and remarkably, discharge capacity reaches  $153 \text{ mAh g}^{-1}$ . The embedded figure in Fig. 3 shows the CV curves of  $\text{LiFePO}_4$  electrode at a scanning rate of  $0.1 \text{ mV s}^{-1}$  at room temperature. The sample exhibited a pair of peaks, an oxidation peak and a reduction peak, which correspond to the two-phase charge–discharge reactions of the  $\text{Fe}^{2+}/\text{Fe}^{3+}$  redox couple, which is in good agreement with the charge-discharge behavior in figure 3. It's worth noting that the  $\text{LiFePO}_4$  sample exhibited an anodic peak at  $3.518 \text{ V}$  and a corresponding cathodic response at  $3.355 \text{ V}$ , with a potential interval of  $0.163 \text{ V}$ , which indicates a higher electrode reaction reversibility and lower polarization for as-synthesized  $\text{LiFePO}_4$  composite.

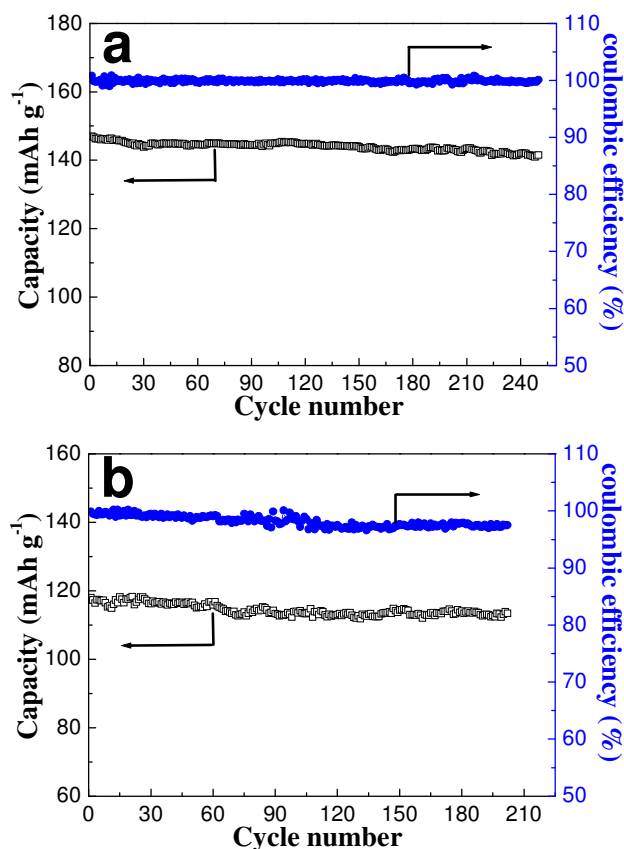


Figure 5 Cycling stability and coulombic efficiency curves of  $\text{LiFePO}_4/\text{C}$  composite: (a) discharging at 1 C rate, (b) discharging at 10 C rate.

Figure 4 demonstrates the rate performance of the as-prepared composite powders. For accurate comparison of the rate performance during discharging, the cells were charged at fixed rate of 0.5 C. then discharged at  $n$  C rate (where  $n = 1, 5, 10, 15, 20, 25$ ). The cutoff voltages were 2.5 and 3.9 V. As shown in figure 4, when the discharge current density increases from 1 C to 25 C, the discharge capacity of  $150, 132, 119, 111, 103$  and  $96 \text{ mAh g}^{-1}$  can still be achieved. Furthermore, even discharging at 25 C rate, it exhibits a significant voltage plateau. This should be very attractive to development of high-power lithium-ion batteries.

The cycling stability and coulombic efficiency of the  $\text{LiFePO}_4/\text{C}$  material are shown in figure 5a and b. The cells were charged to 3.9 V at 1 C rate, and then discharged to 2.5 V at 1 C or 10 C rate. As can be seen from the figure 5a and b, following the 250 cycles discharged at 1 C rate and 202 cycles discharged at 10 C rate, the material retains 96.2% and 96.4% of the original specific capacity, respectively. Meanwhile, the cycle coulombic efficiency is near to 100% up to 250 cycles discharged at 1 C rate and 97.5% up to 202 cycles discharged at 10 C rate, respectively. The excellent rate performance and good cycling performances at different rates of as-prepared  $\text{LiFePO}_4/\text{C}$  composite is undoubtedly related with the nano particle size and spherical morphology, which reduced the diffusion path of lithium ions and electrons, increased the conduc-

tive specific surface and improved the processability of the LiFePO<sub>4</sub> cathode.

#### 4. CONCLUSION

Spherical LiFePO<sub>4</sub>/C nanoparticles have been successfully synthesized using a modified carbothermal reduction method. The LiFePO<sub>4</sub>/C composite shows spherical morphology and nanoscale size. The electrochemical properties of the material are pretty good with excellent rate performance and stable cycling performance at different rates. The prepared composite is the promising material proposed as a cathode for high-power lithium-ion batteries.

#### 5. ACKNOWLEDGMENTS

This work was supported by Doctoral Fund of Shandong Province (BS2009NJ001), the Project of Higher Educational Science and Technology Program of Shandong Province (J10LB56) and the Research Fund of Binzhou University (2008ZDL04).

#### REFERENCES

- [1] M. Armand, J.M. Tarascon, *Nature*, 451, 652 (2008).
- [2] B. Kang, G. Ceder, *Nature*, 458, 190 (2009).
- [3] W.J. Zhang, *J. Power Sources*, 196, 2962 (2011).
- [4] B. Huang, X. Zheng, X. Fan, G. Song, M. Lu, *Electrochim. Acta*, 56, 4865 (2011).
- [5] A.K. Padhi, K.S. Nanjundaswamy, J.B. Goodenough, *J. Electrochem. Soc.*, 144, 1188 (1997).
- [6] A. Yamada, S.C. Chung, K. Hinokuma, *J. Electrochem. Soc.*, 148, A224 (2001).
- [7] S.Y. Chung, J.T. Bloking, Y.M. Chiang, *Nat. Mater.*, 1, 123 (2002).
- [8] P. Subramanya Herle, B. Ellis, N. Coombs, L.F. Nazar, *Nature Mater.*, 3, 147 (2004).
- [9] F. Cheng, W. Wan, Z. Tan, Y. Huang, H. Zhou, J. Chen, X. Zhang, *Electrochim. Acta*, 56, 2999 (2011).
- [10] Y. Liu, C. Cao, *Electrochim. Acta*, 55, 4694 (2010).
- [11] M.M. Doeff, Y. Hu, F. McLarnon, R. Kostecki, *Electrochem. Solid State Lett.*, 6, A207 (2003).
- [12] G.T.-K. Fey, K.P. Huang, H.M. Kao, W. H. Li, *J. Power Sources*, 196, 2810 (2011).
- [13] Y. Yang, X.Z. Liao, Z.F. Ma, B.F. Wang, L. He, Y.S. He, *Electrochem. Commun.*, 11, 1277 (2009).
- [14] J.T. Son, *J. New Mat. Electrochem. Systems*, 13, 301 (2010).
- [15] C.G. Son, H.M. Yang, G.W. Lee, A.R. Cho, V. Aravindan, H.S. Kim, W.S. Kim, Y.S. Lee, *J. Alloys Compd.*, 509, 1279 (2011).
- [16] F. Croce, A.D. Epifanio, J. Hassoun, A. Deptula, T. Olczac, B. Scrosati, *Electrochem. Solid-State Lett.*, 5, A47 (2002).
- [17] Y. Ge, X. Yan, J. Liu, X. Zhang, J. Wang, X. He, R. Wang, H. Xie, *Electrochim. Acta*, 55, 5886 (2010).
- [18] X. Zhao, X. Tang, L. Zhang, M. Zhao, J. Zhai, *Electrochim. Acta*, 55, 5899 (2010).
- [19] D. Wang, H. Li, S. Shi, X. Huang, L. Chen, *Electrochem. Acta*, 50, 2955 (2005).
- [20] X.Z. Liao, Y.S. He, Z.F. Ma, X.M. Zhang, L. Wang, *J. Power*

Sources, 174, 720 (2007).

[21] K.F. Hsu, S.Y. Tsay, B.J. Hwang, *J. Mater. Chem.*, 14, 2690 (2004).